Exciton absorption bleaching studies in ordered $Ga_xIn_{1-x}P$

B. Fluegel, Y. Zhang, H. M. Cheong, A. Mascarenhas, J. F. Geisz, J. M. Olson, and A. Duda
National Renewable Energy Laboratory, Golden, Colorado 80401
(Received 16 December 1996)

Using time-resolved small-signal exciton absorption bleaching at low temperature as a spectroscopic technique, the optical transition energies from all three valence bands in spontaneously ordered $Ga_xIn_{1-x}P$ have been measured with high accuracy. The origin of the bleaching signal and the contributions of reflection, strain, and binding energy are discussed. With three measured energies from each sample, all parameters in the quasicubic perturbation model can be fitted. Good agreement is obtained with a spin-orbit-splitting parameter of 103 meV, nearly independent of the degree of ordering. The ratio of band-gap reduction to crystal-field-splitting parameter is found to be 2.7, slightly higher than previous works. This difference is attributed to a more accurate determination of light-hole-like band-gap energy. [S0163-1829(97)00220-8]

$Ga_xIn_{1-x}P$ is the most extensively studied example of spontaneous long-range atomic ordering in semiconductor alloys.[1] When grown in the [001] direction under special conditions of temperature, growth rate, and substrate misorientation, the cations deposit in alternating [111]-oriented Ga-rich and In-rich planes. An ordering parameter η quantifies the degree of ordering, with $\eta=1$ being a perfect monolayer superlattice, and $\eta=0$ being the random alloy. The band structure of the partially ordered case has been studied by treating the ordering as a perturbation similar to the case of strain, deriving the η dependence of the perturbation parameters, then matching the results to first-principle calculations of the $\eta=1$ and $\eta=0$ cases.[2,3] Band-gap reduction, valence-band splitting (VBS), and a weak dependence of the spin-orbit splitting were predicted as a consequence of ordering.[3] Band-gap reduction is readily observed in photoluminescence (PL); however quantitative measurements of the VBS have been hindered until recently by poor sample quality. In Ref. 4, results were obtained by using modulation spectroscopy to observe relatively sharp features at each band edge, including the spin-orbit band. However, the VBS was still directly resolved only in the samples with the largest ordering, thus requiring a complex fitting procedure. Reference 5 used recent improvements in sample homogeneity to directly observe the VBS by photoluminescence excitation, but the spin-orbit band was not accessible in this technique.

In this paper we use careful substrate removal to prepare a set of free-standing samples with PL linewidths similar to Ref. 5. This opens spontaneous ordering to the relatively unexploited technique of transmission, which can access optical transitions high above the absorption edge. Their spectral resolution is greatly enhanced by using a nonlinear absorption bleaching experiment in which we measure the change in absorption caused by ultrafast excitation. The optical transition energies of the heavy-hole-like (HH), light-hole-like (LH), and spin-orbit (SO) excitons are observed well resolved from their respective absorption bands. Measuring two splittings instead of one allows for independent estimates of the crystal-field-splitting parameter and spin-orbit parameter used in the quasicubic perturbation model.

The samples were grown by atmospheric-pressure organometallic vapor-phase epitaxy on misoriented GaAs substrates. Table I shows specific growth details for each sample. The lattice mismatch between the $Ga_xIn_{1-x}P$ and the substrate was measured by double-crystal x-ray diffraction at room temperature. The composition of the $Ga_xIn_{1-x}P$ samples varied between $x=0.516-0.524$. The sample substrate was removed from a 1 mm area with a chemical etch, leaving a free-standing epilayer supported by its edges over an etched window. All optical measurement were conducted in 5-K He vapor. The measured exciton energies were adjusted to eliminate the contributions of strain and composition[5] using compositions deduced from x-ray measurements. These adjusted values, corresponding to a composition of $Ga_{0.52}In_{0.48}P$, are the presented data.

Optical measurements were performed with an ultrafast laser system consisting of Ti:sapphire-based white-light continuum generator and optical parametric amplifier running at 10 kHz. For the differential absorption (DA) measurement, a 100 fs pump pulse at 2.2 eV excited the sample, creating an electron-hole population that quickly relaxed to the band minima. The quasiequilibrium population modifies the transmission, which was measured by a fs white-light continuum pulse. By chopping the pump beam, the difference in absorbance between pumped and unpumped sample, $\Delta\alpha L$, was directly measured, where L is the sample thickness. The white light was also used to measure linear absorption at the identical sample spot.

TABLE I. Growth parameters and measured HH transition energies for the $Ga_{0.52}In_{0.48}P$ films. T_g is the growth temperature and θ is the orientation of the substrate. The growth rate for all samples was 2 μm/h, and the total film thickness varied from 1 to 2 μm.

T_g (°C)	V/III ratio	θ	E_{HH} (meV)
750	165	$[511]_A$	2013.8
710	165	$[511]_A$	1973.2
690	165	[001], 6°→$[111]_B$	1936.7
670	60	[001], 6°→$[111]_B$	1925.4
670	165	[001], 6°→$[111]_B$	1908.5
650	60	[001], 6°→$[111]_B$	1902.5
670	300	[001], 6°→$[111]_B$	1895.6
650	165	[001], 6°→$[111]_B$	1890.8

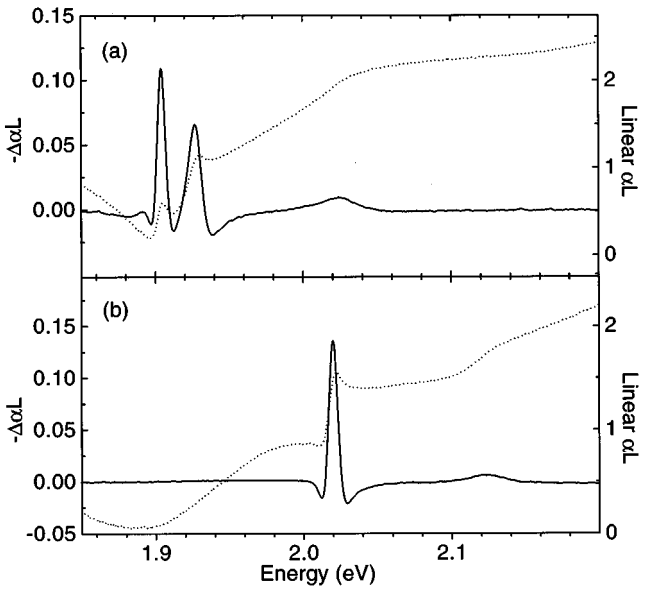

FIG. 1. Linear (dotted curve) and differential (solid curve) absorbance for a 5 K (a) strongly ordered $Ga_xIn_{1-x}P$ sample, and (b) a nominally random alloy. The DA measurement used an excitation pulse of 100 fs, at 2.19 eV with a fluence of 10^{-6} J/cm^2 in a spot size of 250 μm giving an estimated carrier density of 3×10^{16} cm^{-3}. The pump-probe delay was 20 ps.

The dotted curve in Fig. 1(a) shows the linear absorbance αL of a typical $Ga_xIn_{1-x}P$ ordered sample at 5 K with the light polarization oriented parallel to the in-plane projection of the ordering axis. While both HH and LH peaks are marginally resolved from their absorption bands, accurate determination of their splitting would have to model an absorption contribution from the sharply rising tail of the bands. Furthermore, very little precision is possible at the SO peak, where only a very broad shoulder is seen.

In the DA technique, one measures the *change* in linear absorption caused by an optically excited carrier density. As discussed below, using carefully chosen experimental parameters one can observe a signal at the exciton energies only, without contributions from the strong continuum absorption. This is plotted in the solid curve of Fig. 1(a). A positive signal indicates bleaching of the absorption; a negative indicates increased absorption.

If DA is to be an accurate locator of exciton absorption peaks, the signal must be attributed to a mechanism known to be spectrally coincident with the exciton to within the precision of these measurements ($\approx$0.5 meV). As seen in Fig. 1, the bleaching peaks are closely coincident with the linear-absorption peaks, though slightly redshifted, with larger shifts found in samples with broader linewidths. This can be explained by an inhomogeneous broadening, possibly from microscopic ordering or composition fluctuations. The DA signal is caused by carriers that have scattered to the sample's energetically lower regions, while the linear absorption is averaged over the entire sample spot. The bleaching method is still valid microscopically, as all peaks were measured concurrently. As for the bleaching mechanism, we here argue that the signal is entirely excitonic, i.e., from screening of the Coulomb interaction responsible for exciton absorption, or from blocking of those states. Clearly the signal of Fig. 1 is sharply isolated at each band edge, with no obvious bleaching of continuum states. This is consistent with the experiment's long delay time and low excitation density. The density is well below that for exciton ionization, as evident from the small ratio of DA magnitude to linear-absorption magnitude.

Furthermore, the earlier dynamics of the signal (not shown) contain only limited evidence for blocking of continuum or exciton states. Continuum blocking by the hot carriers should appear as an early, broadband, rapidly cooling bleaching. Phase-space filling of the HH exciton could be recognized from a slow (ps) increase of the HH signal during the final stages of cooling. Both of these effects are seen with excitation densities higher than that used in Fig. 1. In contrast, for the excitation density of Fig. 1, there are no resolvable dynamics beyond a fast initial rise of the exciton peaks and a slow reduction in the induced absorption below the HH. The long delay time used, 20 ps, was chosen to avoid this slight effect of carrier cooling. Longer delay times do not change the peak locations.

From these considerations we assign the DA bleaching peaks in Fig. 1 primarily to screening, with a possible smaller contribution from phase-space filling. Small renormalizations of the exciton energy are possible from both mechanisms,[6,7] but in this small signal regime, they are expected to be much less than the binding energy. This is supported by the spectral shape of the signal: the spectral shape of the DA is a sensitive measure of the exciton energy shift, and shifts result in a characteristic dispersive-shaped odd-symmetric signal. In contrast, the signals of Fig. 1 are symmetric, indicating a bleaching accompanied by a small broadening. The exciton transition energies are therefore the peak energies seen in the DA. By using exciton bleaching, the energies have been located even in samples where the linear absorption peaks are not well resolved from the continua, or in the case of the SO peak, not seen at all. Figure 1(b) is the result of an identical measurement on a nominally random alloy. In sharp contrast to the first sample, the valence-band splitting is completely unresolved, and the $E_{SO}-E_{HH}$ splitting has decreased as well.

The influence of multiple-reflection peaks on the measurement of the HH peak was considered. To avoid the chance of strain or other unknown effects from further processing, the etched epilayers were not antireflection coated, resulting in strong modulation of the below-band-edge transmission. A small pump-induced change in the refractive index can produce similar modulation in the DA signal. To check that the sloping reflection just below E_{HH} did not affect our measurement of that energy, the measurement was rechecked at several sample positions of different thickness. The peak energy varied slightly with sample position, but did not correlate with the reflection phase. Further confirmation came from wedge-shaped samples that averaged out interference effects. Peak positions were not consistently different between wedged and flat regions.

Since our analysis of the exciton data deals with the energy difference between valence bands at $k=0$, the variations of exciton binding energies between valence bands and with degree of ordering need to be considered. Using the anisotropic effective masses calculated in Refs. 8 and 9, and the binding energy results of Ref. 10, the $Ga_xIn_{1-x}P$ binding

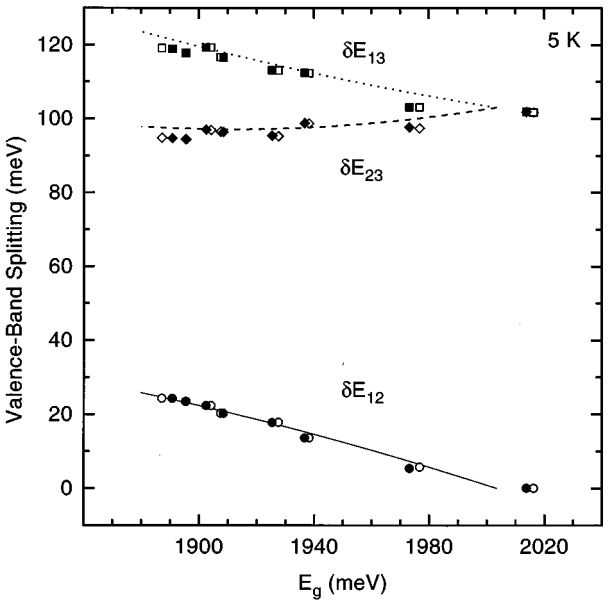

FIG. 2. Energy gap differences for 5 K $Ga_xIn_{1-x}P$ plotted against the HH peak energy. Experimental conditions were identical to Fig. 1. Discrete points: Experimentally measured SO splitting (δE_{13}), VBS (δE_{12}), and their difference (δE_{23}). Open points are original data, solid points are data corrected for lattice and composition mismatch through x-ray measurements. The precision of the DA measurement at a fixed sample location was 0.3 meV for the HH and LH peaks, and 0.7 meV for the SO peak. Curves: Calculated results from Eqs. (1)–(3) and parameters Δ_{SO} and Δ_{CF} fit to the experimental points.

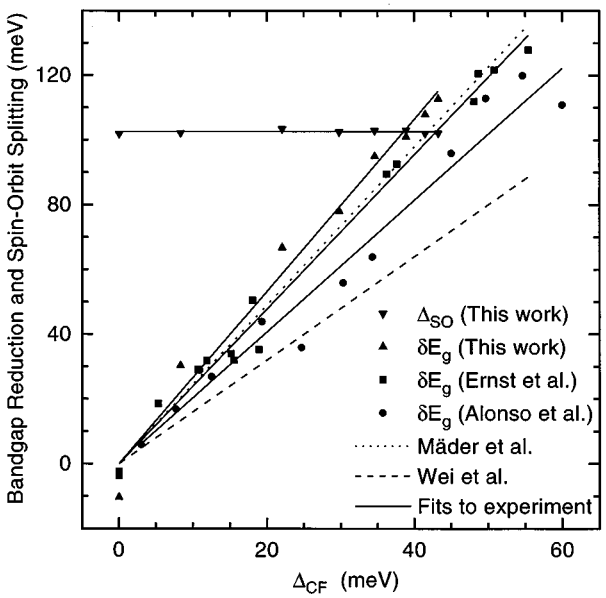

FIG. 3. Discrete points: extracted parameters from experimental data points of this work and others. Triangles: SO-splitting parameter and band-gap reduction plotted against crystal-field-splitting parameter for this work. Band-gap reduction was referenced to a fitted value of $E_{HH}=2003$ meV for the completely random material. Also plotted is band-gap reduction for Ref. 5 (squares) and Ref. 4 (circles). Solid curves: linear fits to the three experiments. Dashed and dotted curves: theoretical predictions from Refs. 2 and 14.

energy was estimated for the three valence bands, and over the limited range of ordering in these samples. The results were constant to within $\pm 3\%$, which is within our experimental reproducibility. Therefore the measured exciton energy differences $E_{LH}-E_{HH}$, $E_{SO}-E_{HH}$, and $E_{SO}-E_{LH}$ are interpreted as the energy difference between zone-center valence bands, δE_{12}, δE_{13}, and δE_{23}, respectively. These values, from eight samples exhibiting various degrees of ordering, are plotted in Fig. 2 as a function of $E_g \equiv$(band gap$-$binding energy), the useful experimental parameter. This is qualitatively similar to the results of Ref. 4. These experimentally measured VBS and SO splitting are the result of order-induced mixing between the more fundamental crystal-field splitting and spin-orbit coupling. Therefore, a quantitative comparison with other experimental and theoretical works is best accomplished by extracting splitting parameters of the perturbation model.

Treating the CuPt ordering as a perturbation to the zinc-blende structure, the valence bands can be described by the so called quasicubic model.[11,3] The three band-edge states are

$$E_1 = a + \frac{\Delta_{CF}}{3}, \tag{1}$$

$$E_2 = a - \frac{1}{2}\left(\Delta_{SO} + \frac{\Delta_{CF}}{3}\right) + \frac{1}{2}\left[\left(\Delta_{SO} - \frac{\Delta_{CF}}{3}\right)^2 + \frac{8\Delta_{CF}^2}{9}\right]^{1/2}, \tag{2}$$

$$E_3 = a - \frac{1}{2}\left(\Delta_{SO} + \frac{\Delta_{CF}}{3}\right) - \frac{1}{2}\left[\left(\Delta_{SO} - \frac{\Delta_{CF}}{3}\right)^2 + \frac{8\Delta_{CF}^2}{9}\right]^{1/2}, \tag{3}$$

with a, Δ_{SO}, and Δ_{CF} all quadratic functions of the degree of ordering. a is an averaged shift of the valence band, Δ_{CF} is the so-called crystal-field-splitting parameter that is the valence-band splitting without the spin-orbit interaction, and Δ_{SO} is the spin-orbit interaction parameter, which we also take to be order dependent. We note that the functional forms of Eqs. (1)–(3) are valid only when the change to the spin-orbit interaction from the rhombohedral distortion is ignored.[8]

For each sample, using Eqs. (1)–(3) and the experimental results δE_{13} and δE_{23}, we can solve for Δ_{CF} and Δ_{SO}. In practice, we use a numerical solution of a Hamiltonian (similar to Ref. 12) that includes strain and composition dependence of band structure due to the small deviation of the composition from its lattice-matched value $x_0=0.52$. Figure 3 shows the band-gap reduction and Δ_{SO} versus Δ_{CF}. Δ_{SO} is nearly independent of the ordering in the order parameter range covered by this work, with a mean value of $\Delta_{SO}=102.6\pm0.2$ meV. The piezomodulated-reflectivity study of Alonso *et al.* found $\Delta_{SO}\approx 103$ meV for a disordered sample,[4] while theory[13] predicts a weak quadratic enhancement of Δ_{SO} from 100 meV for nominally random alloy, to 110 meV for fully ordered.

The ratio $\delta E_g/\Delta_{CF}$ is found from Fig. 3 to be 2.66 ± 0.15, which is larger than the theoretical results 2.45 of

Mäder and Zunger[14] and 1.60 of Wei, Laks, and Zunger.[3] It is also larger than the experimental results 2.36 ± 0.06 of Ernst *et al.*,[5] and 2.03 ± 0.13 of Alonso *et al.*[4] (analyzed in Ref. 8). While the data of Alonso *et al.* are less accurate due to the sample quality and use of a complex fitting procedure, the data of Ernst *et al.* are obtained from PL excitation (PLE) measurements on samples with comparable quality. However, as mentioned earlier, because the splitting δE_{12} is relatively small, direct measurement of the splitting from PLE or linear absorption is less accurate, and especially when the ordering is weak, the two peaks are hardly resolvable in these measurements. In fact, if we use the δE_{12} values from our *linear*-absorption measurement and following the same procedure of Ernst *et al.*, we get almost the same value of $\delta E_g/\Delta_{\mathrm{CF}}=2.46\pm0.17$. Our experimental results deviate from the theoretical curves, but it appears more close to the result of Mäder and Zunger (pseudopotential in the local-density approximation) than that of Wei, Laks, and Zunger (linearized augmented plane wave in the local-density approximation).[15] Plotted with our experimental data points in Fig. 2 are curves calculated using Eqs. (1)–(3) with $\Delta_{\mathrm{SO}}=103$ meV and $\delta E_g/\Delta_{\mathrm{CF}}=2.66$, which have been obtained from Fig. 3.[16]

In conclusion, DA is used for a systematic study of the valence band and spin-orbit splitting in $Ga_xIn_{1-x}P$ samples as a function of ordering. The DA method has the advantage of providing sharp features at the HH, LH, and SO excitons, even when they are not well resolved from the continua. With the exceptions of our nominally random sample and the least ordered sample, the HH and LH peaks were always entirely separated from each other, with no need for a fitting procedure. Using the measured peak separations, we have made a quantitative investigation of the applicability of the quasicubic model to all the three valence bands, and studied the ordering effect on the spin-orbit interaction.

We would like to thank C. Kramer for growth of the samples. This work was supported by the Office of Energy Research, Material Science Division of the DOE under Contract No. DE-AC36-83CH10093.

[1] A. Zunger and S. Mahajan, in *Handbook on Semiconductors, 2nd ed.*, edited by S. Mahajan (Elsevier, Amsterdam, 1994), Vol. 3, Chap. 19, p. 1399.

[2] D. B. Laks, S.-H. Wei, and A. Zunger, Phys. Rev. Lett. **69**, 3766 (1992).

[3] S.-H. Wei, D. B. Laks, and A. Zunger, Appl. Phys. Lett. **62**, 1937 (1993).

[4] R. G. Alonso, A. Mascarenhas, G. S. Horner, K. A. Bertness, S. R. Kurtz, and J. M. Olsen, Phys. Rev. B **48**, 11 833 (1993).

[5] P. Ernst, C. Geng, F. Scholz, H. Schweizer, Y. Zhang, and A. Mascarenhas, Appl. Phys. Lett. **67**, 2347 (1995).

[6] H. Haug and S. Schmitt-Rink, J. Opt. Soc. Am. B **2**, 1135 (1985).

[7] S. Schmitt-Rink, D. S. Chemla, and D. A. B. Miller, Phys. Rev. B **32**, 6601 (1985).

[8] Y. Zhang and A. Mascarenhas, Phys. Rev. B **51**, 13 162 (1995).

[9] A. Franceschetti, S.-H. Wei, and A. Zunger, in *Optoelectronic Materials—Ordering, Composition Modulation, and Self-Assembled Structures*, edited by E. D. Jones *et al.*, MRS Symposium Proceedings No. 417 (Materials Research Society, Pittsburgh, 1996), p. 103.

[10] P. G. Harper and J. A. Hilder, Phys. Status Solidi **26**, 69 (1968).

[11] J. J. Hopfield, J. Phys. Chem. Solids **15**, 97 (1960).

[12] S.-H. Wei and A. Zunger, Phys. Rev. B **49**, 14 337 (1994).

[13] S.-H. Wei, A. Franceschetti, and A. Zunger, in *Optoelectronic Materials—Ordering, Composition Modulation, and Self-Assembled Structures* (Ref. 9), p. 3.

[14] K. A. Mäder and A. Zunger, Appl. Phys. Lett. **64**, 2882 (1994); Phys. Rev. B **51**, 10 462 (1995).

[15] The difference in these values was recently discussed in Ref. 13 and reflects the uncertainty in the $\Gamma_{1C}-L_{1C}$ energy splitting in the random alloy at $x=\frac{1}{2}$.

[16] In our analysis, we have assumed that after the small window of substrate is removed, the lattice of the epilayer is still constrained by the surrounding substrate. If this assumption is incorrect, the composition-only correction would change our results of $\delta E_g/\Delta_{\mathrm{CF}}$ by -1%, and leave the mean Δ_{SO} unchanged.